Comparison between interferometric and piezoelectric readout of tuning fork vibrations in quartz-enhanced photoacoustic spectroscopy

P. Patimisco[a], S. Zou[b], S. dello Russo[a], A. Zifarelli[a], A. Sampaolo[a], M. Giglio[a], H. Rossmadl[c], V. Mackowiak[c], Alex Cable[d], D. Iannuzzi[b], and V. Spagnolo[a]

[a] PolySense Lab - Dipartimento Interateneo di Fisica, University and Politecnico of Bari, Via Amendola 173, Bari, Italy
[b] Department of Physics and Astronomy, VU University Amsterdam, Amsterdam, Netherlands
[c] Thorlabs GmbH, Hans-Boeckler-Straße 6, 85221 Dachau, Germany
[d] Thorlabs, Inc., 56 Sparta Ave., Newton, 07860, USA

ABSTRACT

We report on a comparison between the piezoelectric and interferometric readouts of vibrations in quartz tuning forks (QTFs) when employed as sound wave transducers in quartz-enhanced photoacoustic trace gas sensors. We demonstrate the possibility to properly design the QTF geometry to enhance interferometric readout signal with respect to the piezoelectric one and vice versa. When resonator tubes are acoustically coupled with the QTFs, signal-to-noise ratio enhancements are observed for both readout approaches. These results open the way to the implementation of optical readout of QTF vibrations in applications where external electromagnetic field could distort the piezoelectric signal.

Keywords: quartz-enhanced photoacoustic spectroscopy, gas sensing, tuning fork, interferometry.

1. INTRODUCTION

Quartz tuning forks (QTFs) are used as sound wave transducers in quartz-enhanced photoacoustic spectroscopy (QEPAS) for gas sensing applications [1-6]. When the intensity-modulated laser beam is focused between prongs, sound waves deflect them and the QTF anti-symmetrical flexural mode is excited [7-10]. The QTF is a piezoelectric element that converts the deflection of prongs into an electrical signal. Progresses in QTF designs have been aimed to identify figures of merit to optimizing a QEPAS sensor performance. Extensive theoretical and experimental investigations have been performed to study the acousto-electro properties of QTFs [11, 12] as well as energy loss mechanism occurring in a vibrating prong [13, 14] and the spatial distribution of the stress field when prongs are forced to vibrate [15]. These studies provided the guidelines to design QTFs optimized for QEPAS sensing: decrease the resonance frequency while keeping high the quality factor [12].

The deflection can be also optically readout using an interferometric laser system. Laser interferometers can detect displacements down to few picometers [16, 17]. Interferometric systems are mainly composed by a near-infrared diode laser and a photodetector. M. Kohring et al. exploited the optical readout for QTF-based photoacoustic sensing by using quartz and silicon tuning forks, reaching QTF thermal noise as ultimate noise level [18-19]. In addition, they demonstrated that piezoelectric and optical readout reach comparable sensitivity and detection limits, with the same experimental conditions [20]. However, literature lacks of a detailed and extensive investigation of QTF properties regarding the optimization of the interferometric readout of prong vibrations.

Here, we compared the interferometric and piezoelectric readouts of QTF vibrations and demonstrated that the QTF geometry can be properly designed to enhance a selected readout mode. For piezoelectric readout, the QTF showing the highest performance has a T-shape prong geometry and a resonance frequency of 12.45 kHz [12]. Among custom QTFs employed so far in QEPAS [11, 21-24], the QTF with the largest vibration amplitude has a resonance frequency of 3.44 kHz. Both QTFs were implemented in a QEPAS sensor and tested for the detection of water vapor concentration in the room air. The signal-to-noise ratio of piezoelectric readout results was ~ 40% higher than the interferometric one when the T-QTF was employed. Conversely, an interferometric signal ~ 50% times larger than the piezoelectric one has been measured when implementing the 3.44 kHz-QTF. When the QTFs were acoustically coupled with dual-tube resonator

systems [25], both readout techniques showed a signal-to-noise ratio enhancement. Although the largest signal-to-noise ratio has been achieved with piezoelectric readout, interferometric approach could be preferred in applications involving high intensity electromagnetic fields that distort the piezoelectric signal and affect its signal-to-noise ratio.

2. QUARTZ TUNING FORKS FOR PIEZOELECTRIC AND OPTICAL READOUT

In QEPAS, the laser beam should pass through the gap between the two prongs of the QTF to produce a QTF signal. In traditional QEPAS sensors, the laser beam is aligned to be perpendicular to the QTF plane [1-2, 26]. The T-shape prong geometry demonstrated the best QEPAS performance. With respect to standard rectangular shape, T-shaping the prongs geometry allows an increase of the strain field on the prong base, providing an enhancement of the photoacoustic response in terms of signal-to-noise ratio [6, 12]. Compared to QTF with rectangular shape, the resonance frequency of the T-shaped QTF is slightly reduced while the resonance Q-factor is not affected. The T-shaped QTF (T-QTF) used in this work is schematized in Fig. 1a. The prong has a full length of $L = L_1 + L_2$ = 9.4 mm (L_1 = 2.4 mm), a crystal thickness of T = 250 μm, and W_1 and W_2 are 2 mm and 1.4 mm, respectively.

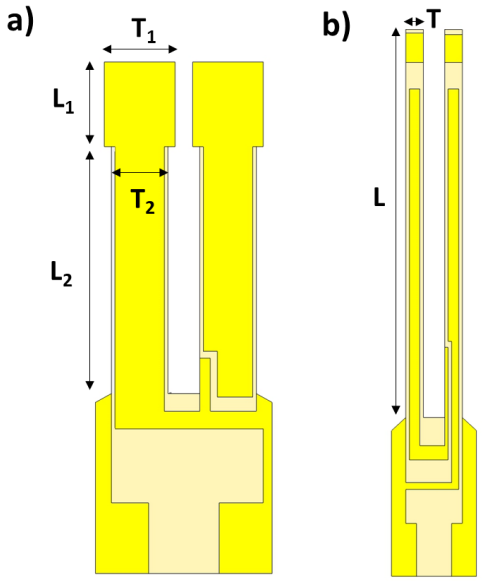

Figure 1. Schematic view of T-QTF (a) and I-QTF geometry (b).

The optical readout is based on measurement of deflections of a cantilever via an optical interferometric system. The larger the vibration amplitude of the prong, the higher the optical readout signal. The amplitude of prong vibration can be related by the QTF resonance and electrical properties by the relation:

$$a = \sqrt{\frac{QVI}{2\pi fk}} \tag{1}$$

where Q is the QTF quality factor, V is the voltage across the QTF and I the generated piezo-current, f is the resonance frequency and k is the spring constant. Among all custom QTFs discussed in [11], the QTF showing the highest vibration amplitude calculated by using Eq. (1) is the one having prong length of L = 11.0 mm, prong thickness of T = 0.5 mm and crystal width of W = 0.25 mm (I-QTF). The geometry of the I-QTF is schematized in Fig. 1b. The resonance properties of both QTFs, namely the resonance frequency and the quality factor, have been measured by using the experimental setup depicted in Fig. 2a. A function generator with a resolution of 2 mHz was used to provide a sinusoidal voltage excitation to the QTFs. The piezoelectric current is then converted to an output voltage by means of the trans-impedance amplifier and then the lock-in amplifier demodulates the signal at the same frequency as the waveform generator. The

resonance curve of the fundamental mode of T-QTF is reported in Fig. 2b. The resonance curve of the I-QTF excited at the fundamental and first overtone mode are reported in Fig. 2c and Fig. 2d, respectively.

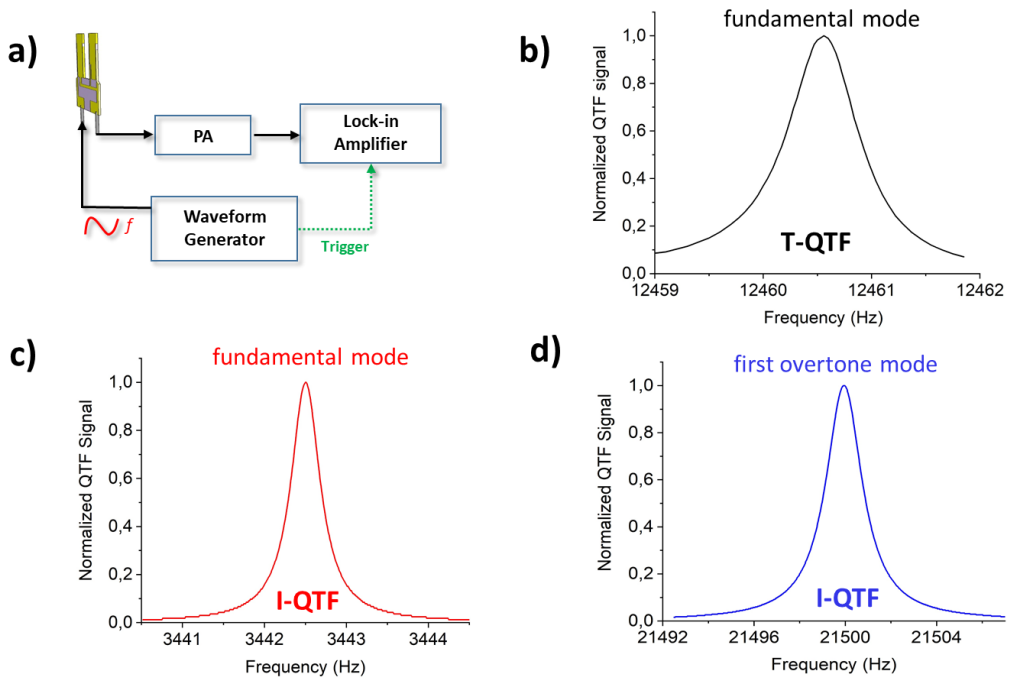

Figure 2. (a) Sketch of the setup measurement of QTF resonance curve via electrical excitation. PA: transimpedance preamplifier. (b) Resonance curve of T-QTF at the fundamental mode. (c) Resonance curve of I-QTF at the fundamental mode. (d) Resonance curve of I-QTF at the first overtone mode.

The resonance curves were fitted using a Lorentzian function to determine the peak resonance frequency, f_0, and the full-width-half-maximum value, Δf. Hence, the quality factor results $Q = f_0/\Delta f$. In Table 1, the calculated resonance frequencies as well as quality factor values are listed.

Table 1. Experimental resonance properties for T-QTF (fundamental mode) and I-QTF (fundamental and first overtone mode): f_0 (resonance frequency), Δf (the full width at half maximum value of the QTF resonance curve), Q (quality factor).

	f_0 (Hz)	Δf (Hz)	Q
T-QTF fundamental mode	12460.55	0.80	15570
I-QTF fundamental mode	3442.50	0.83	4150
I-QTF first overtone mode	21499.94	1.77	12100

All measurements have been performed at atmospheric pressure and room temperature.

3. EXPERIMENTAL SETUP

The QEPAS system with piezoelectric and optical readout methods for a vibrating QTF is sketched in Fig. 3a and 3b, respectively.

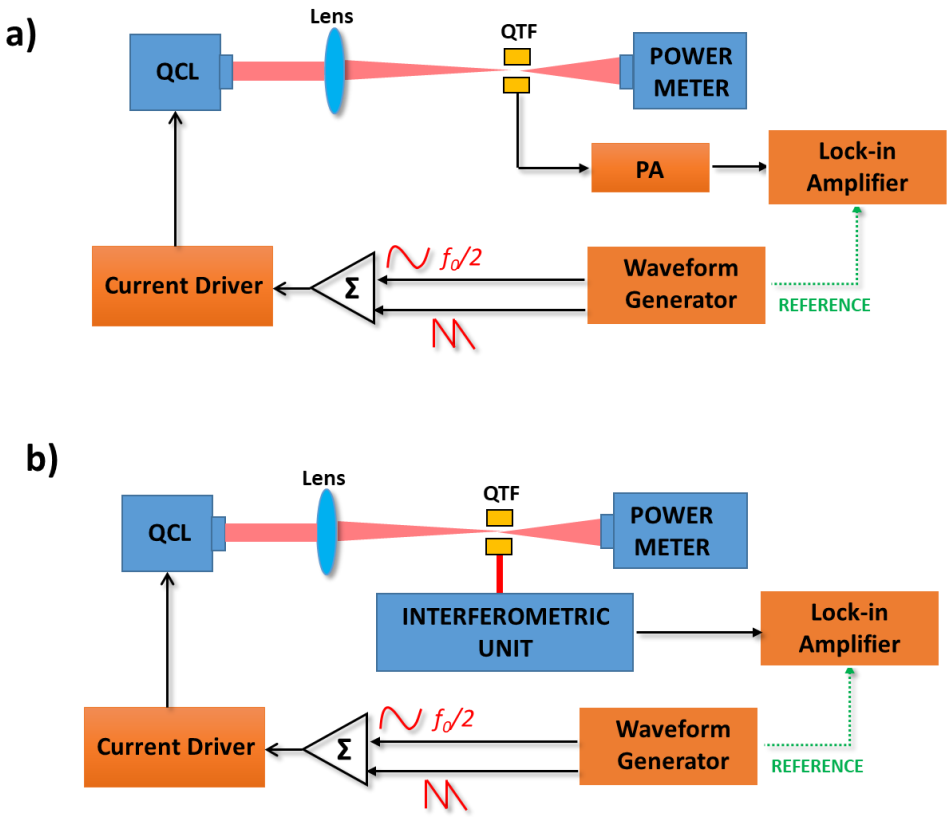

Figure 3. QEPAS system with piezoelectric (a) and optical (b) readout.

The beam of a quantum cascade laser (QCL) was focused between the QTF prongs by using a ZnSe lens with a focal length of 50 mm. The platform allowed an easy interchange between T-QTF and I-QTF. Both QEPAS and optical readout were performed in wavelength modulation and second harmonic detection: the laser beam was intensity-modulated at half of the QTF resonance frequency by adding a sinusoidal dither to the current driver [27]. Then, for piezoelectric readout, the QTF signal was demodulated at the QTF resonance frequency. By applying a low frequency ramp at the laser current driver, the wavelength emission was tuned to scan across a water absorption features peaked at 1296.71 cm^{-1} at atmospheric pressure. For the optical readout, a commercial fiber coupled interferometer (OP1550 V3, Optics11) based on Fabry–Perot interference was employed. A near-infrared laser hits the lateral surface of one QTF prong, at a distance of ~ 500 µm. Gold layers deposited on QTF prongs allowed high reflectivity for an efficient optical readout. The laser beam pointed close to the top where the lateral displacement of the prong is largest. The back-reflected light were sent to an interferometric unit to generate a voltage signal proportional to the interference light intensity. The voltage signal was demodulated at the QTF resonance frequency. All measurements were performed in air at atmospheric pressure, with a stable concentration of water vapor constantly monitored by an in-line hygrometer.

4. RESULTS

Figure 4 shows the piezoelectric and the optical signal for T-QTF excited at the fundamental mode, acquired while the laser wavelength was scanned across the selected water absorption line.

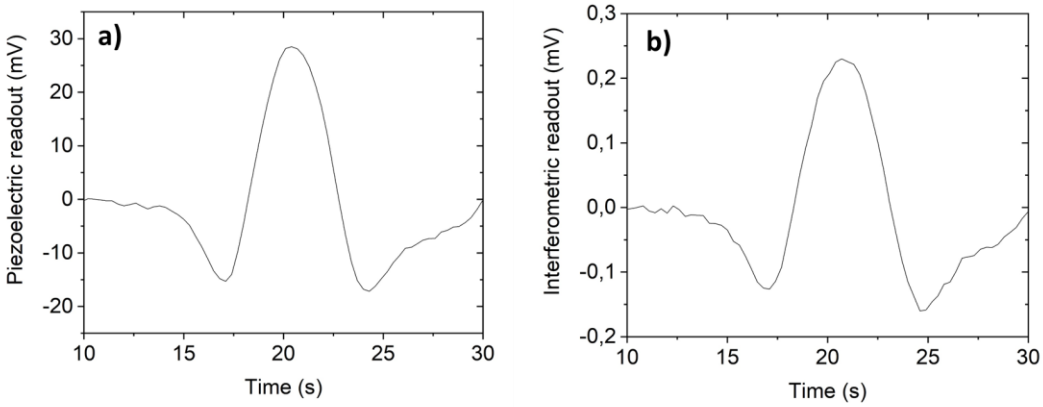

Figure 4. QEPAS spectral scan of water absorption line acquired with T-QTF excited at the fundamental mode with piezoelectric (a) and interferometric (b) readout.

Both readout methods are suitable to reconstruct the water absorption feature. Far from the two strong absorption peaks, both interferometric and piezoelectric readouts are background-free. To compare the sensing performance, the signal-to-noise ratio (SNR) has to be calculated. With the same experimental conditions, the spectral scan have been acquired by using I-QTF excited at the fundamental and first overtone mode. The calculated SNRs are summarized in Fig. 5, when both readout methods are used.

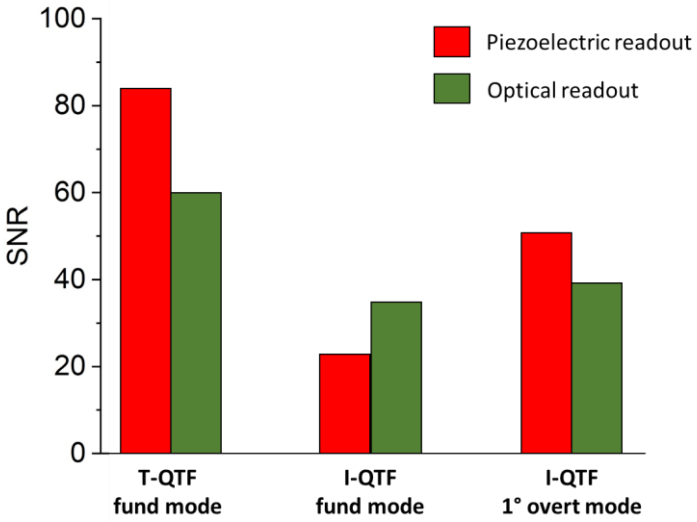

Figure 5. Signal-to-noise ratios measured for I-QTF (at the fundamental and first overtone mode) and T-QTF (at the fundamental mode), when piezoelectric or interferometric readouts are selected.

With T-QTF, the piezoelectric readout results ~40% more sensitive than the interferometric one. This can be ascribed to the fact that T-QTF was properly designed to offer high QEPAS performance for piezoelectric readout. Conversely, I-QTF excited at the fundamental mode showed best performance when the optical readout was used. This proves that the QTF geometry could be optimized when interferometric measurement systems are to be adopted. The straightforward approach is to choose a prong geometry maximizing the vibration amplitude. When I-QTF is excited at the first overtone mode, the SNR is 2.2 times higher than that obtained when the I-QTF operated at the fundamental mode. This demonstrates the possibility to increase the piezoelectric readout sensitivity through the use of QTFs optimized to operate at the first resonance overtone [28]. When optical readout is used, the SNR is comparable with that measured

when I-QTF vibrates at the fundamental mode, demonstrating that the interferometric technique is not influenced by the flexural resonance mode of the I-QTF.
In QEPAS, the QTF is usually acoustically coupled with a pair of resonator tubes, acting as amplifiers for the sound wave [25, 26]. The QTF is typically positioned between the tubes to probe the acoustic vibration excited in the absorbing gas contained inside the tubes. T-QTF have been coupled with a pair of tubes having length of 10 mm and an internal diameter of 1.59 mm. With piezoelectric readout, a SNR is enhanced of ~16 compared to the bare T-QTF, while a SNR enhancement of ~13 with respect to bare T-QTF have been measure when piezoelectric readout is adopted. Thereby, when implementing resonator tubes, the T-QTF piezoelectric detection is more sensitive than the interferometric one.

5. CONCLUSIONS

In this work, we compared the piezoelectric and interferometric readouts of vibrations in quartz tuning forks (QTFs) when used in QEPAS sensors. By properly selecting the QTF prong geometry, it is possible to enhance interferometric readout signal with respect to the piezoelectric one or vice versa. Two different QTFs (T-QTF and I-QTF) have been implemented in a QEPAS sensor with the laser source tuned to detect a water absorption line in air at atmospheric pressure. Both readout methods have implemented in the QEPAS setup. When the bare T-QTF is excited at the fundamental mode, SNR of piezoelectric readout results ~ 40% higher than that of interferometric one. Conversely, when the I-QTF is excited at the fundamental mode, the SNR of the interferometric readout is ~ 50% times larger than the piezoelectric one. When operating at the first overtone mode, the I-QTF provide a piezoelectric SNR ~2.2 times higher than when operating at the fundamental mode, while the interferometric SNR remains almost the same.

6. AKNOWLEDGMENTS

The authors from Dipartimento Interateneo di Fisica di Bari acknowledge financial support from THORLABS GmbH, within the joint research laboratory PolySense.

REFERENCES

[1] Patimisco, P., Sampaolo, A., Zheng, H., Dong, L., Tittel, F.K. and Spagnolo V., “Quartz enhanced photoacoustic spectrophones exploiting custom tuning forks: a review,” Adv. Phys. X 2, 169-187 (2016).
[2] Patimisco, P., Sampaolo, A., Dong, L., Tittel, F.K., Spagnolo V., “Recent advances in quartz enhanced photoacoustic sensing,” Appl. Phys. Rev., 011106 (2018).
[3] Sampaolo, A., Patimisco, P., Giglio, M., Chieco, L., Scamarcio, G., Tittel, F.K., and Spagnolo, V., “Highly sensitive gas leak detector based on a quartz-enhanced photoacoustic SF_6 sensor,” Opt. Express 24, 15872-15881 (2016).
[4] Patimisco, P., Borri, S., Galli, I., Mazzotti, D., Giusfredi, G., Akikusa, N., Yamanishi, M., Scamarcio, G., De Natale, P., and Spagnolo, V., “High finesse optical cavity coupled with a quartz-enhanced photoacoustic spectroscopic sensor,” Analyst 140, 736–743 (2015).
[5] Giglio, M., Patimisco, P., Sampaolo, A., Scamarcio, G., Tittel, F. K., and Spagnolo, V., “Allan Deviation Plot as a Tool for Quartz-Enhanced Photoacoustic Sensors Noise Analysis,” IEEE Trans. Ultrason. Ferroelect. Freq. Control 63, 555-560 (2016).
[6] Giglio, M., Elefante, A., Patimisco, P., Sampaolo, A., Sgobba, F., Rossmadl, H., Mackowiak, V., Wu, H., Tittel, F.K., Dong, L., and Spagnolo, V., "Quartz-enhanced photoacoustic sensor for ethylene detection implementing optimized custom tuning fork-based spectrophone." Opt. Express 27, 4271-4280 (2019).
[7] Sampaolo, A., Csutak, S., Patimisco, P., Giglio, M., Menduni, G., Passaro, V., Tittel, F.K., Deffenbaugh, M., and Spagnolo, V., “Methane, ethane and propane detection using a compact quartz enhanced photoacoustic sensors and a single interband cascade laser”, Sens. Act. B Chem. 282, 952-960 (2019).
[8] Giglio, M., Patimisco, P., Sampaolo, A., Zifarelli, A., Blanchard, R., Pfluegl, C., Witinski, M.F., Vakhshoori, D., Tittel, F.K., and Spagnolo, V., Nitrous oxide quartz-enhanced photoacoustic detection employing a broadband distributed-feedback quantum cascade laser array,” Appl. Phys. Lett. 113, 171101 (2018).
[9] Viciani, S., Siciliani de Cumis, M., Borri, S., Patimisco, P., Sampaolo, A., Scamarcio, G., De Natale, P., D'Amato, F., and Spagnolo, V., “A quartz-enhanced photoacoustic sensor for H_2S trace-gas detection at 2.6 μm,” Appl. Phys. B 119, 21-27 (2014).

[10] Elefante, A., Giglio, M., Sampaolo, A., Menduni, G., Patimisco, P., Passaro, V.M., Wu, H., Rossmadl, H., Mackowiak, V., Cable, A. and Tittel, F.K., 2019. Dual-Gas Quartz-Enhanced Photoacoustic Sensor for Simultaneous Detection of Methane/Nitrous Oxide and Water Vapor. Anal. Chem. 91, 12866-12873 (2019).
[11] Patimisco, P., Sampaolo, A., Dong, L., Giglio, M., Scamarcio, G., Tittel, F.K., and Spagnolo, V., "Analysis of the electro-elastic properties of custom quartz tuning forks for optoacoustic gas sensing," Sensor Actuat. B-Chem. 227, 539-546 (2016).
[12] Patimisco, P., Sampaolo, A., Giglio, M., Dello Russo, S., Mackowiak, V., Rossmadl, H., Cable, A., Tittel, F.K. and Spagnolo, V., "Tuning forks with optimized geometries for quartz-enhanced photoacoustic spectroscopy," Opt. Express 27, 1401-1415 (2019).
[13] Patimisco, P., Sampaolo, A., Mackowiak, V., Rossmadl, H., Cable, A., Tittel, F.K., and Spagnolo, V., "Loss Mechanisms Determining the Quality Factors in Quartz Tuning Forks Vibrating at the Fundamental and First Overtone Modes," IEEE Trans. Ultrason. Ferroelect. Freq. Control. 65, 1951-1957 (2018).
[14] Giglio, M., Menduni, G., Patimisco, P., Sampaolo, A., Elefante, A., Passaro, V., and Spagnolo, V., "Damping Mechanisms of Piezoelectric Quartz Tuning Forks Employed in Photoacoustic Spectroscopy for Trace Gas Sensing," Phys. Status Solidi A 216, 1800552 (2019).
[15] Patimisco, P., Sampaolo, A., Giglio, M., Mackowiak, V., Rossmadl, H., Gross, B., Cable, A., Tittel, F.K. and Spagnolo, V., "Octupole electrode pattern for tuning forks vibrating at the first overtone mode in quartz-enhanced photoacoustic spectroscopy," Opt. Lett. 43, 1854-1857 (2018).
[16] Pisani, M., Yacoot, A., Balling, P., Bancone, N., Birlikseven, C., Çelik, M., Flügge, J., Hamid, R., Köchert, P., and Kren, P., "Comparison of the performance of the next generation of optical interferometers," Metrologia 49, 455-467 (2012).
[17] Shao, L. and Gorman, J. J., "Pulsed laser interferometry with sub-picometer resolution using quadrature detection," Opt. Express 24, 17459-17469 (2016).
[18] Köhring, M., Pohlkötter, A., Willer, U., Angelmahr, M., and Schade, W., "Tuning fork enhanced interferometric photoacoustic spectroscopy: a new method for trace gas analysis," Appl. Phys. B 102, 133-139 (2011).
[19] Köhring, M., Willer, U., Böttger, S., Pohlkötter, A., and Schade, W., "Fiber-Coupled Ozone Sensor Based on Tuning Fork-Enhanced Interferometric Photoacoustic Spectroscopy," IEEE J. Sel. Top. Quant. 18, 1566-1572 (2012).
[20] Köhring, M., Böttger, S., Willer, U., and Schade, W., "Temperature effects in tuning fork enhanced interferometric photoacoustic spectroscopy," Opt. Express 18 20911- 20922 (2013).
[21] Zheng, H., Dong, L., Patimisco, P., Wu, H., Sampaolo, A., Yin, X., Li, S., Ma, W., Zhang, L., Yin, W., Xiao, L., Spagnolo, V., Jia, S., Tittel, F.K., "Double antinode excited quartz-enhanced photoacoustic spectrophone," Appl. Phys. Lett. 110, 021110 (2017).
[22] Wu, H., Yin, X., Dong, L., Pei, K., Sampaolo, A., Patimisco, P., Zheng, H., Ma, W., Zhang, L., Yin, W., Xiao, L., Spagnolo, V., Jia, S., Tittel, F.K., "Simultaneous dual-gas QEPAS detection based on a fundamental and overtone combined vibration of quartz tuning fork," Appl. Phys. Lett. 110, 121104 (2017).
[23] Zheng, H., Dong, L., Sampaolo, A., Wu, H., Patimisco, P., Ma, W., Zhang, L., Yin, W., Xiao, L., Spagnolo, V., Jia, S., and Tittel, F.K., "Overtone resonance enhanced single-tube on-beam quartz enhanced photoacoustic spectrophone," Appl. Phys. Lett. 109, 111103 (2016).
[24] Patimisco, P., Spagnolo, V., Vitiello, M. S., Tredicucci, A., Scamarcio, G., Bledt, C. M., and Harrington, J. A., "Coupling external cavity mid-IR quantum cascade lasers with low loss hollow metallic/dielectric waveguides," Appl. Phys. B 108, 255–260 (2012).
[25] Dello Russo, S., Giglio, M., Sampaolo, A., Patimisco, P., Menduni, G., Wu, H., Dong, L., Passaro, V.M.N., and Spagnolo, V., "Acoustic coupling between resonator tubes in quartz-enhanced photoacoustic spectrophones employing a large prong spacing tuning fork," Sensors 19, 4109 (2019).
[26] Dong, L., Kosterev, A.A., Thomazy, D., Tittel, F.K., "QEPAS spectrophones: design, optimization, and performance," Appl. Phys. B 100, 627–635 (2010).
[27] Patimisco, P., Sampaolo, A., Bidaux, Y., Bismuto, A., Scott, M., Jiang, J., Muller, A., Faist, J., Tittel, F.K., and Spagnolo, V., "Purely wavelength- and amplitude-modulated quartz-enhanced photoacoustic spectroscopy," Opt. Express 24, 25943-25954 (2016).
[28] Tittel, F.K., Sampaolo, A., Patimisco, P., Dong, L., Geras, A., Starecki, T., and Spagnolo, V., "Analysis of overtone flexural modes operation in quartz-enhanced photoacoustic spectroscopy," Opt. Express 24, A682-A692 (2016).